

Thermodynamic analysis on the formation mechanism of $\text{MgO}\cdot\text{Al}_2\text{O}_3$ spinel type inclusions in casing steel

Hai-yan Tang and Jing-she Li

School of Metallurgical and Ecological Engineering, University of Science and Technology Beijing, Beijing 100083, China

(Received: 21 December 2008; revised: 19 January 2009; accepted: 7 February 2009)

Abstract: $\text{MgO}\cdot\text{Al}_2\text{O}_3$ spinel type inclusions in casing steel were analyzed by scanning electron microscope (SEM) and energy dispersive spectrometer (EDS). The results show that there are three forms. One is pure $\text{MgO}\cdot\text{Al}_2\text{O}_3$ spinel, another is the composite oxide of the Mg-Al-Ca-Si-O system, and the third is the complex with oxide as a core covered by sulfide. The formation mechanisms were studied. The influences of slag basicity and vacuum degree on the magnesium content during the vacuum treatment of molten steel and furnace lining in molten steel were calculated with the coexistence theory of slag structure. The results show that the magnesium content increases with the increase in slag basicity and aluminum content in molten steel, and decreases with the increase in CO partial pressure.

Keywords: magnesium-aluminum spinel; basicity; theoretical model; formation mechanism

1. Introduction

Casing is an important material for oil fields. It can reinforce the wall of an oil well and protect the hole of the oil well, and its destruction can lead to the failure throughout the well. Therefore, not only high strength, uniform and stable quality, strong corrosion, and wear resistance are required for casings, but also the capacity to support all kinds of loads such as pulling, pressing, twisting, and bending is needed.

The tests show that the $\text{MgO}\cdot\text{Al}_2\text{O}_3$ spinel type inclusion in the tube is one of the important factors affecting the quality of the casing. Therefore, it is very necessary to study its formation mechanism and effect factors to control it in production.

There have been some investigations [1-4] on the mechanism of $\text{MgO}\cdot\text{Al}_2\text{O}_3$ spinel in stainless steel melts, but systematical theory analyses are few. Because it is difficult to measure and calculate the activity of every component of a multicomponent slag, the activities of some components are often assumed to be 1 in most investigations. In fact, their activities are impossible to be 1 for these components at

high temperature.

The coexistence theory is used to calculate the activity of the slag component. Based on the thermodynamic data collected by predecessors, the theory deals with many problems such as oxidizing ability of slag, manganese distribution between slag and steel, desulphurization and dephosphorization ability of slag, and activity of molten salt and aqueous solution, achieving uniform results with reality [5-13]. In this theory, the mass action concentration of the component is activity. In the paper, according to the actual production, the mass action concentration model of $\text{CaO}-\text{MgO}-\text{FeO}-\text{Al}_2\text{O}_3-\text{SiO}_2$ slag systems was chosen to calculate the activities of components relative to the formation of $\text{MgO}\cdot\text{Al}_2\text{O}_3$ spinel, and further to study the influence law of slag components, vacuum treatment, and furnace lining on the magnesium content in molten steel.

2. Forms of $\text{MgO}\cdot\text{Al}_2\text{O}_3$ spinel type inclusions observed in casing steel

The composition of casing steel in the research (wt%) is 0.39 C, 0.22 Si, 1.52 Mn, 0.015 P, 0.007 S, 0.10 Mo, 0.020 Al, 0.12 V, 0.25 Cu, and 0.04 Cr.

There are three kinds of forms of MgO·Al₂O₃ spinel in casing steel. One is dependent spherical MgO·Al₂O₃, mainly containing Mg, Al, and O elements as shown in Fig. 1. Another is the composite oxide inclusion with Mg, Al, Si, Ca,

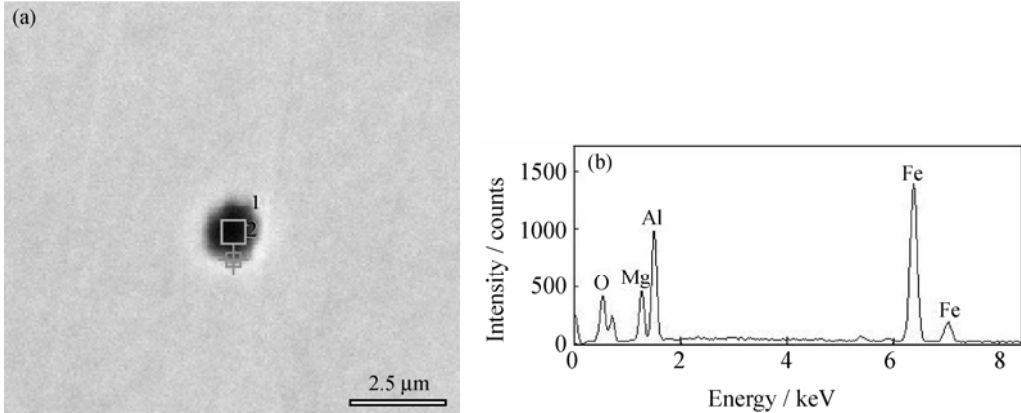


Fig. 1. Morphology (a) and energy spectrum (b) for point 1 of pure MgO·Al₂O₃ spinel.

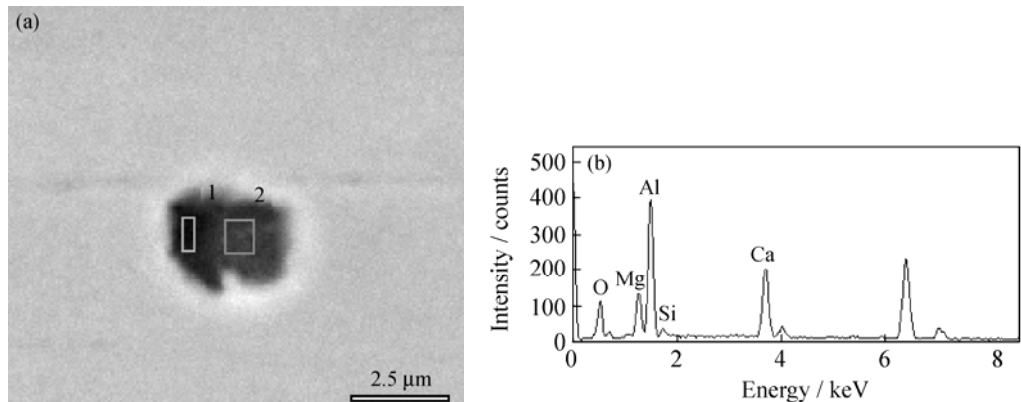


Fig. 2. Morphology (a) and energy spectrum (b) for point 1 of a composite oxide inclusion.

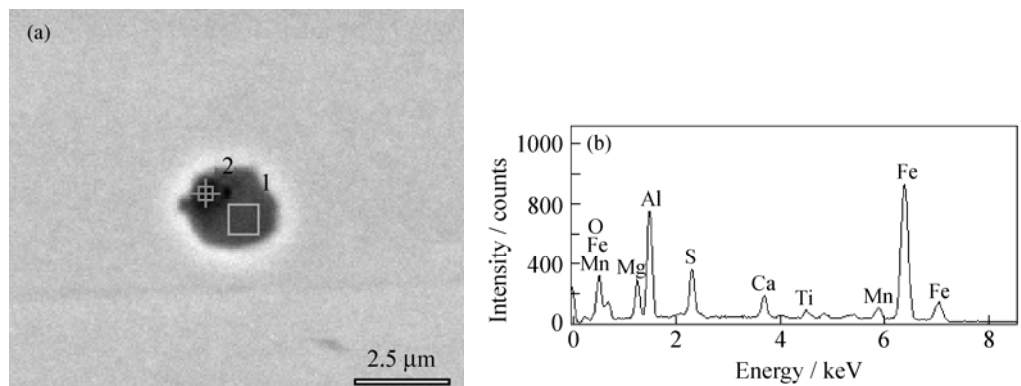


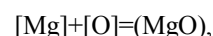
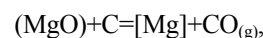
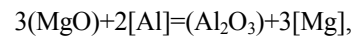
Fig. 3. Morphology (a) and energy spectrum (b) for point 1 of MgO·Al₂O₃ covered by sulphide.

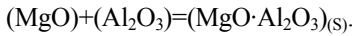
3. Formation mechanism of MgO·Al₂O₃ spinel

There are mainly four sources for magnesium in molten steel: (1) MgO in slag is reduced by aluminum in molten steel; (2) MgO in slag is reduced by carbon in vacuum treatment; (3) MgO in lining is reduced by carbon in vacuum treatment; (4) MgO in lining is reduced by aluminum

and O as shown in Fig. 2. The third is MgO·Al₂O₃ spinel as a core wrapped with sulphide as shown in Fig. 3. The energy spectra given in Figs. 1-3 are all for point 1.

in molten steel. Then magnesium in molten steel is oxidized into MgO, which combines with Al₂O₃ into MgO·Al₂O₃ spinel. The reactions are expressed as [14]





3.1. Theoretical model of the influence of slag compositions on the magnesium content

Ref. [15] showed that the composition of inclusions was close to that of slag at steel-slag equilibrium. In production, there hardly existed an absolute equilibrium, but there existed a local quasi-equilibrium state between molten steel and inclusion, molten steel and slag, lining and slag, and lining and molten steel. The composition of inclusions was influenced by the slag and lining compositions to a great degree. Conversely, through controlling the compositions of the slag and lining, the composition of the inclusion can be controlled.

The following reactions occur in molten steel:



$$\Delta G_1^\Theta = -5009908 + 122.9 T, \text{ J/mol} \quad [16],$$



$$\Delta G_2^\Theta = -1206220 + 390.39 T, \text{ J/mol} \quad [16],$$

where ΔG_1^Θ and ΔG_2^Θ are the Gibbs free energies of reactions (1) and (2), respectively; and T is the temperature.

According to the coexistence theory of slag structure and thermodynamic equilibrium, the following equations are obtained:

$$K_{MgO} = \frac{N_{MgO}}{a_{Mg} \cdot a_O} = \frac{N_{MgO}}{[MgO][O]f_{Mg}f_O} \quad (3)$$

$$K_{Al_2O_3} = \frac{N_{Al_2O_3}}{a_{Al}^2 \cdot a_O^3} = \frac{N_{Al_2O_3}}{[Al]^2[O]^3f_{Al}^2f_O^3} \quad (4)$$

$$\lg \{[Mg] \cdot [O]\} =$$

$$\lg N_{MgO} - \frac{26212.04}{T} - \lg f_{Mg} - \lg f_O + 6.43 \quad (5)$$

$$\lg \{[Al]^2 \cdot [O]^3\} =$$

$$\lg N_{Al_2O_3} - \frac{63109}{T} - 2\lg f_{Al} - 3\lg f_O + 20.42 \quad (6)$$

$$\lg f_i = \sum_j e_i^j[j],$$

where K_{MgO} and $K_{Al_2O_3}$ are the equilibrium constants of reactions (1) and (2), respectively; N_{MgO} and $N_{Al_2O_3}$ are the mass action concentrations of MgO and Al_2O_3 in slag, respectively; $[Mg]$, $[O]$, and $[Al]$ are the mass fractions of Mg,

O, and Al in molten steel, respectively; f_i is the activity coefficient of component i ; and a_i is the activity of component i .

Substituting the chemical components of casing steel, it is derived as: $f_{Al}=1.062$, $f_{Mg}=0.767$, $f_O=0.492$ (1873 K).

Theoretical models of the influence of slag compositions on the magnesium content at 1873 K are derived by substituting activity coefficients into Eqs. (5) and (6):

$$\lg \{[Mg] \cdot [O]\} = \lg N_{MgO} - 7.1419 \quad (7)$$

$$\lg \{[Al]^2 \cdot [O]^3\} = \lg N_{Al_2O_3} - 12.4034 \quad (8)$$

3.2. Effect of slag compositions on [Al]-[O] equilibrium

It can be seen from Eq. (6), if the slag action is neglected, $N_{Al_2O_3} = 1$, then

$$\lg \{[Al]^2 \cdot [O]^3\} = -\frac{63109}{T} - 2\lg f_{Al} - 3\lg f_O + 20.42.$$

If the slag action is considered,

$$\begin{aligned} \lg \{[Al]^2 \cdot [O]^3\} = \\ \lg N_{Al_2O_3} - \frac{63109}{T} - 2\lg f_{Al} - 3\lg f_O + 20.42. \end{aligned}$$

In the paper, thirteen groups of slags were designed with their basicities ($B=[CaO]/[SiO_2]$, where [CaO] and [SiO₂] are the mass fractions of CaO and SiO₂ in slag, respectively) from 1.0 to 7.0, and N_{MgO} and $N_{Al_2O_3}$ were calculated by the method in Ref. [17]. The programs and results are shown in Table 1. It is seen that basicity has a large influence on the activity of Al_2O_3 . The latter decreases with the former increasing, which is in agreement with the results in the references. When the basicity increases from 1.0 to 7.0, the mass action concentration of Al_2O_3 decreases from 0.0811 to 0.00063. As a result, it is not appropriate to assume that the activity of Al_2O_3 in a multi-component slag is 1 in some references.

Table 2 lists the calculated [Al]-[O] equilibrium values at 1873 K when considering and not considering the slag action. From Table 2, the aluminum content in molten steel and slag basicity have large effects on the oxygen content. The higher the aluminum content, the lower the oxygen content. When not considering the slag action, if $[Al]=0.02\text{wt\%}$, $[O]=9.96 \times 10^{-6}$; if $[Al]=0.05\text{wt\%}$, $[O]=5.41 \times 10^{-6}$. Therefore, the control of the aluminum content is necessary to produce high purity clean steel. It can also be seen that oxygen contents when considering and not considering the slag action at the same aluminum content.

Not considering the slag action, when [Al]=0.02wt%, [O]=9.96×10⁻⁶; whereas considering the slag action, when [Al]=0.02wt%, [O] varies from 4.31×10⁻⁶ to 0.90×10⁻⁶ with the slag basicity increasing from 1.0 to 6.0. As a result, slag

composition has a large effect on the oxygen content in molten steel and high basicity slag is favorable for decreasing the oxygen content of molten steel.

Table 1. Designed slag composition and the calculated values of N_{MgO} and $N_{\text{Al}_2\text{O}_3}$

<i>B</i>	Slag composition / wt%					N_{MgO}	$N_{\text{Al}_2\text{O}_3}$
	CaO	SiO ₂	MgO	Al ₂ O ₃	FeO		
1.0	42.25	42.25	5.00	10.00	0.50	0.0103	0.08110
1.5	50.70	33.80	5.00	10.00	0.50	0.0063	0.05800
2.0	56.33	28.17	5.00	10.00	0.50	0.0250	0.01320
2.5	60.36	24.14	5.00	10.00	0.50	0.0765	0.00440
3.0	63.38	21.12	5.00	10.00	0.50	0.1200	0.00250
3.5	65.72	18.78	5.00	10.00	0.50	0.1463	0.00180
4.0	67.60	16.90	5.00	10.00	0.50	0.1501	0.00140
4.5	69.14	15.36	5.00	10.00	0.50	0.1440	0.00110
5.0	70.42	14.08	5.00	10.00	0.50	0.1382	0.00095
5.5	71.50	13.00	5.00	10.00	0.50	0.1332	0.00083
6.0	72.43	12.07	5.00	10.00	0.50	0.1290	0.00074
6.5	73.23	11.27	5.00	10.00	0.50	0.1254	0.00068
7.0	73.94	10.56	5.00	10.00	0.50	0.1222	0.00063

Table 2. [Al]-[O] equilibrium values at 1873 K when considering and not considering the slag action

[Al] / wt%	Considering the slag action	[O] / 10 ⁻⁶							
		Not considering the slag action							
		<i>B</i> =1.0	<i>B</i> =1.5	<i>B</i> =2.0	<i>B</i> =2.5	<i>B</i> =3.0	<i>B</i> =4.0	<i>B</i> =5.0	<i>B</i> =6.0
0.001	73.37	31.26	28.40	17.34	12.02	9.96	8.21	7.20	6.65
0.005	25.09	10.86	9.71	5.93	4.11	3.41	2.81	2.46	2.27
0.010	15.81	6.84	6.12	3.74	2.59	2.15	1.77	1.55	1.43
0.014	12.63	5.47	4.89	2.99	2.07	1.71	1.41	1.24	1.14
0.020	9.96	4.31	3.85	2.35	1.63	1.35	1.11	0.98	0.90
0.025	8.58	3.72	3.32	2.03	1.41	1.16	0.96	0.84	0.78
0.030	7.60	3.29	2.94	1.80	1.25	1.03	0.85	0.75	0.69
0.040	6.27	2.72	2.43	1.48	1.03	0.85	0.70	0.62	0.57
0.050	5.41	2.34	2.09	1.28	0.89	0.73	0.60	0.53	0.49
0.060	4.79	2.07	1.85	1.13	0.78	0.65	0.54	0.47	0.43

3.3. Effect of the aluminum content on the magnesium content in molten casing steel

The [Al]-[Mg] relationship at 1873 K is derived from Eqs. (7) and (8) as

$$[\text{Mg}] = 10^{-3.0074} \cdot N_{\text{MgO}} \cdot \left\{ [\text{Al}]^2 / N_{\text{Al}_2\text{O}_3} \right\}^{1/3} \quad (9)$$

For eight groups of slags chosen from Table 1, the calculated [Al]-[Mg] relationship is plotted in Fig. 4. From Fig. 4, the magnesium content in molten steel increases with the aluminum content increasing. When *B* is in the range of 1.0-1.5, the trend of increase is not obvious. Whereas when *B* is in the range of 2.5-6.0, the trend of increase is very ob-

vious, which may lead to the increase in the possibility of forming magnesium-aluminum spinel.

3.4. Effect of slag basicity and the Al₂O₃ content on the magnesium content in molten casing steel

Fig. 5 shows the relationship between slag basicity and [O] in the condition of (MgO)=0.05wt%, (FeO)=0.5wt%, and [Al]=0.02wt%, where (MgO) and (FeO) are the mass fractions of MgO and FeO in slag, respectively. Fig. 6 shows the relationship between slag basicity and [Mg] in the condition of (MgO)=5wt%, (FeO)=0.5wt%, and [Al]=0.02wt%. It can be seen that [O] decreases and [Mg] increases with the basicity increasing. And the higher the

Al_2O_3 content in slag, the higher the [O] and the lower the [Mg]. with the (Al_2O_3) increasing, the activity decreases when basicity increases. According to the [Al]-[O] equilibrium, [O] decreases, further [Mg] increases. When $(\text{Al}_2\text{O}_3)=10\text{wt}\%$ and $B=2.5$, it can be seen $[O]=1.8\times 10^{-6}$ and $[\text{Mg}]=3.8\times 10^{-7}$ in Fig. (5) and Fig. (6), which are closer to the measured values.

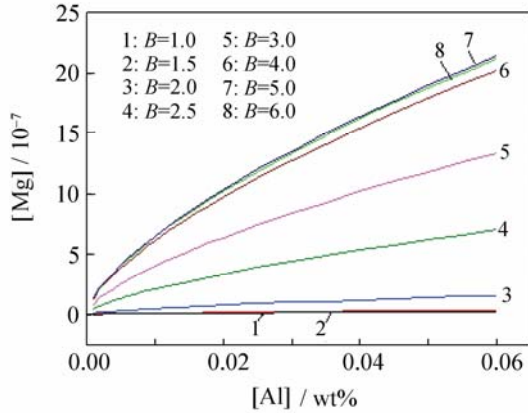


Fig. 4. [Al]-[Mg] equilibrium at different basicities.

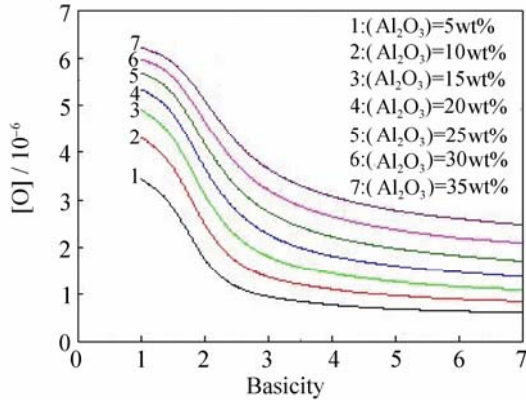
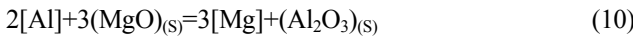


Fig. 5. Relationship between slag basicity and [O] in the condition of $(\text{MgO})=5\text{wt}\%$, $(\text{FeO})=0.5\text{wt}\%$, and $[\text{Al}]=0.02\text{wt}\%$.

3.5. Effect of refractory on the magnesium content in casing steel

At present, most refractories contain MgO. When the aluminum in molten steel is higher, MgO in the refractory will be reduced, and further magnesium-aluminum spinel will be formed. The equations can be expressed as



$$\Delta G^\Theta = 296752.4 + 21.69 T, \text{ J/mol.}$$

For refractory, $N_{\text{MgO}}=1$,

$$K = \left\{ a_{[\text{Mg}]}^3 \cdot N_{\text{Al}_2\text{O}_3} \right\} / a_{[\text{Al}]}^2 = \left\{ f_{\text{Mg}}^3 [\text{Mg}]^3 \cdot N_{\text{Al}_2\text{O}_3} \right\} / (f_{\text{Al}}^2 [\text{Al}]^2).$$

At $T=1873 \text{ K}$,

$$[\text{Mg}] = 10^{-3.1358} [\text{Al}]^{2/3} / N_{\text{Al}_2\text{O}_3}^{1/3} \quad (11)$$

This is the theoretical model of aluminum reducing MgO in the lining.

According to the actual compositions of slag, assuming $(\text{MgO})=5\text{wt}\%$, $(\text{Al}_2\text{O}_3)=10\text{wt}\%$, $(\text{FeO})=0.5\text{wt}\%$, $B=0.5, 2, 3, 4, 6$, and $T=1873 \text{ K}$, $N_{\text{Al}_2\text{O}_3}$ was calculated under different basicities using the mass action concentration model of the CaO-MgO-FeO-Al₂O₃-SiO₂ slag systems. Then it was substituted into Eq. (11) to obtain the relationship of the magnesium content and the aluminum content as shown in Fig. 7. It can be seen that the action on the lining increases with the aluminum content increasing, which makes the magnesium content increase. At the same aluminum content, the magnesium content in molten steel is higher when considering the slag action than not considering it. With the increase in slag basicity, the magnesium content increases. This is because slag has the ability of absorbing Al₂O₃ inclusions. The higher the slag basicity, the stronger the ability of absorbing Al₂O₃ inclusions, thus the reaction of Eq. (10) is moved to the right side and the magnesium content increases.

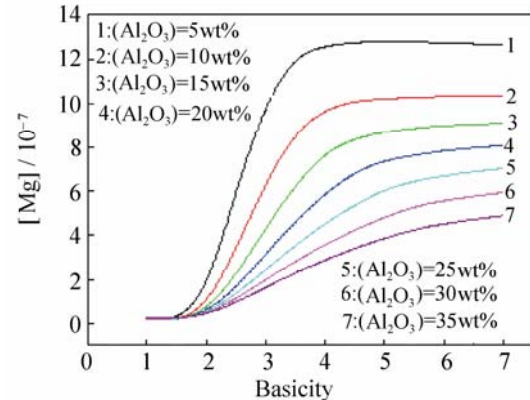
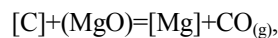


Fig. 6. Relationship between slag basicity and [Mg] in the condition of $(\text{MgO})=5\text{wt}\%$, $(\text{FeO})=0.5\text{wt}\%$, and $[\text{Al}]=0.02\text{wt}\%$.

3.6. Effect of vacuum carbon on magnesium content

The equilibrium reaction of vacuum carbon reducing MgO can be expressed as



$$\Delta G^\Theta = 722976.29 - 281.59 T, \text{ J/mol.}$$

$$K = (P_{\text{CO}} a_{\text{Mg}}) / (a_{\text{MgO}} a_{\text{C}}) = \left\{ P_{\text{CO}} f_{\text{Mg}} [\text{Mg}] \right\} / \left\{ N_{\text{MgO}} f_{\text{C}} [\text{C}] \right\},$$

where K is the equilibrium constant of the reaction, P_{CO} is the partial pressure of CO.

Substituting $f_c=1.139$, $f_{\text{Mg}}=0.767$, and $[\text{C}]=0.39\text{wt}\%$, it

can be obtained that at 1873 K,

$$\lg P_{\text{CO}}[\text{Mg}] = \lg N_{\text{MgO}} - 5.70284.$$

When MgO in lining is reduced by carbon, $N_{\text{MgO}}=1$, then

$$[\text{Mg}] = 10^{-5.70284} / P_{\text{CO}} \quad (12)$$

When MgO in slag is reduced,

$$[\text{Mg}] = 10^{-5.70284} \cdot N_{\text{MgO}} / P_{\text{CO}} \quad (13)$$

Eqs. (12) and (13) are the theoretical models of vacuum carbon reducing MgO . Table 3 lists the magnesium content values in molten steel when carbon reduces MgO in the lining. It can be seen that the magnesium content increases rapidly with the partial pressure of CO decreasing. When $P_{\text{CO}}>5066.25 \text{ Pa}$, $[\text{Mg}] \approx 0$.

Table 3. [Mg] values at different P_{CO} when carbon reduces MgO in lining

$P_{\text{CO}} / \text{Pa}$	10.1325	101.325	506.625	1013.25	5066.25	10132.5	50662.5	101325
$[\text{Mg}] / 10^{-7}$	1980	198	39.6	19.8	3.96	1.98	0.396	0.198

Table 4 shows the relationship of slag basicity and the CO partial pressure and the magnesium content when carbon reduces MgO in slag at $(\text{MgO})=5\text{wt\%}$, $(\text{Al}_2\text{O}_3)=10\text{wt\%}$, and $(\text{FeO})=0.5\text{wt\%}$. It can be seen that the magnesium content at first increases with basicity increasing at the same CO partial pressure. The magnesium content reaches the largest value when $B=4$. Later on, the magnesium content decreases with the slag basicity increasing. At the same basicity, the magnesium content decreases with the CO partial pressure

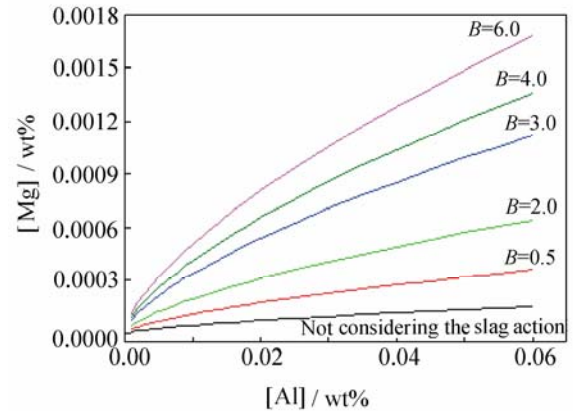


Fig. 7. Relationship of $[\text{Mg}]\text{-}[\text{Al}]$ for Al reducing MgO in the lining.

increasing. Comparing Tables 3 and 4, when the CO partial pressures are 101.325 and 506.625 Pa, carbon reduces MgO in the lining, the magnesium contents are 19.8×10^{-6} and 3.96×10^{-6} , respectively. Whereas the corresponding values are only $(0.214\text{-}29.750) \times 10^{-7}$ when reducing MgO in slag. As a result, there is a larger effect on the magnesium content when carbon reduces MgO in lining than in slag under vacuum condition.

Table 4. Relationship of slag basicity and magnesium content at different P_{CO}

B	$[\text{Mg}] / 10^{-7}$						
	101.325 Pa	506.625 Pa	1013.25 Pa	5066.25 Pa	10132.5 Pa	50662.5 Pa	101325 Pa
0.5	1.070	0.214	0.107	0.0214	0.0107	0.00214	0.00107
1.0	2.042	0.408	0.204	0.0408	0.0204	0.00408	0.00204
2.0	4.956	0.991	0.496	0.0991	0.0496	0.00991	0.00496
3.0	23.787	4.757	2.379	0.4757	0.2379	0.04757	0.02379
4.0	29.750	5.951	2.975	0.5951	0.2975	0.05951	0.02975
5.0	27.395	5.479	2.740	0.5479	0.2740	0.05479	0.02740
6.0	25.571	5.114	2.557	0.5114	0.2557	0.05114	0.02557
7.0	24.223	4.845	2.422	0.4845	0.2422	0.04845	0.02422

4. Conclusions

(1) There are three kinds of existence forms for $\text{MgO}\cdot\text{Al}_2\text{O}_3$ spinel in casing steel.

(2) The formation of $\text{MgO}\cdot\text{Al}_2\text{O}_3$ spinel in casing steel can be interpreted as that, MgO in slag or lining is reduced

by aluminum in molten steel or by carbon under vacuum to form magnesium. Then magnesium combines with oxygen to form MgO . Finally, MgO reacts with Al_2O_3 to form $\text{MgO}\cdot\text{Al}_2\text{O}_3$ spinel.

(3) The theoretical models for the influence of slag component, vacuum degree, and refractory on the magnesium

content in molten steel are established. The calculations show that the magnesium content increases with the increase in slag basicity and the aluminum content, and decreases with the increase in the CO partial pressure.

Acknowledgement

The authors are very grateful for the help of Prof. Guo-guang Cheng in applying the structure model of slag.

References

- [1] S.K. Jo, B. Song, and S.H. Kim, Thermodynamics on the formation of spinel ($MgO\cdot Al_2O_3$) inclusion in liquid iron containing chromium, *Metall. Mater. Trans. B*, 33(2002), p.709.
- [2] H.P. Joo, Formation mechanism of spinel-type inclusions in high-alloyed stainless steel melts, *Metall. Mater. Trans. B*, 38(2007), p.657.
- [3] W.Y. Cha, D.S. Kim, Y.D. Lee, and J.J. Pak, A thermodynamic study on the inclusion formation in ferritic stainless steel melt, *ISIJ Int.*, 44(2004), No.7, p.1134.
- [4] H.P. Joo and S.K. Dong, Effect of $CaO\cdot Al_2O_3\cdot MgO$ slags on the formation of $MgO\cdot Al_2O_3$ inclusions in ferritic stainless steel, *Metall. Mater. Trans. B*, 36(2005), p.495.
- [5] J. Zhang, Coexistence theory of slag structure and its application to calculation of oxidizing capability of slag melts, *J. Iron Steel Res. Int.*, 10(2003), No.1, p.1.
- [6] J. Zhang, Application of the coexistence theory of slag structure to multicomponent slag systems, [in] *Proceedings of the 4th International Conference on Molten Slags and Fluxes*, Sendai, 1992, p.244.
- [7] J. Zhang, The equilibrium of manganese between $FeO\cdot MnO\cdot MgO\cdot SiO_2$ slag system and liquid iron, *J. Univ. Sci. Technol. Beijing* (in Chinese), 14(1992), No.5, p.496.
- [8] J. Zhang, Application of the law of mass action in combination with the coexistence theory of slag structure to multicomponent slag systems, *Acta Metall. Sin. Engl. Lett.*, 14(2001), No.3, p.177.
- [9] J. Zhang, Applicability of law of mass action to distribution of manganese between slag melts and liquid iron, *Trans. Non-ferrous Met. Soc. China*, 11(2001), No.5, p.778.
- [10] J. Zhang, Applicability of mass action law to sulphur distribution between slag melts and liquid iron, *J. Univ. Sci. Technol. Beijing*, 9(2002), No.2, p.90.
- [11] J. Zhang, Applicability of annexation principle to the study of thermodynamic properties of ternary molten salts $CaCl_2\cdot MgCl_2\cdot NaCl$, *Rare Met.*, 23(2004), No.3, p.209.
- [12] H.J. Guo, W.J. Zhao, and X.M. Yang, Calculating models of mass action concentrations for $NaBr(aq)$, $LiNO_3(aq)$, $HNO_3(aq)$ and $KF(aq)$ solutions, *J. Univ. Sci. Technol. Beijing*, 14(2007), No.3, p.204.
- [13] H.J. Guo, W.J. Zhao, L. Li, and X.M. Yang, A universal thermodynamic model of calculating mass action concentrations of components in strong electrolyte binary aqueous solutions, *Chin. J. Process Eng.* (in Chinese), 7(2007), No.2, p.45.
- [14] H.Y. Tang, *Study on Inclusion Control for N80 Casing Steel Produced by EAF-LF-VD-CC Process* [Dissertation] (in Chinese), University of Science and Technology Beijing, Beijing, 2008, p.155.
- [15] H. Suito, Thermodynamics on control of inclusions compositions in ultra-clean steel, *ISIJ Int.*, 36(1996), No.5, p.528.
- [16] C.M. Yu, X.D. Miu, C.M. Shi, et al., Behaviour of spinel $MgO\cdot Al_2O_3$ inclusions in ball bearing steel, *J. Univ. Sci. Technol. Beijing* (in Chinese), 27(2005), Suppl.2, p.37.
- [17] J. Zhang, *Calculating Thermodynamics of Metallurgical Melts*, Metallurgical Industry Press, Beijing, 2007, p.390.